J. Fluid Mech. (1999), *vol.* 384, *pp.* 281–292. Printed in the United Kingdom

A note on the optimum profile of a sprayless planing surface

By DMITRI V. MAKLAKOV

Chebotarev Institute of Mathematics and Mechanics, Kazan State University, Universitetskaya, 17, Kazan, 420008, Russia

(Received 21 March 1997 and in revised form 3 November 1998)

The paper presents an exact analytical solution to the problem of finding the optimum profile of a two-dimensional plate which planes on a water surface without spray formation and maximizes the lift force. The lift is maximized under the only isoperimetric constraint of fixed total arclength of the plate. The exact solution is compared with approximate analytical and numerical results by Wu & Whitney (1972). The shape of the optimum plate turns out to be technically unrealizable because of small, tightly wound spirals near the end points. It was shown numerically that cutting off small segments near the end points leads on the one hand to insignificant change in the lift force and on the other hand to a non-separating boundary layer along the remaining part of the optimum plate.

1. Introduction

Let us consider the problem formulated by Wu & Whitney (1972). A curved plate AB of length $2L$ planes on the free surface of an ideal incompressible fluid. In the body frame of reference the free-stream velocity is V_0 in the positive x-direction. The Froude number $Fr = V_0/(2gl)^{1/2}$, based on the chord length $2l$ and the gravitational constant g, is assumed to be so large that the effect of gravity may be neglected. The flow in the physical z-plane is shown in figure 1. The origin of the coordinate system is located at the point O which divides the plate into two parts with equal lengths L. On the free streamlines CA and BC the velocity is constant and equal to V_0. The problem is to find the shape of the plate which maximizes the lift F_y under the isoperimetric constraints of fixed chord $2l$ and total arclength $2L$.

An important feature of the above formulation is that the planing surface satisfies the so-called 'smooth entry' condition, when the width of the spray sheet near the leading edge equals zero. Cumberbatch (1958) was the first to explore this flow regime that for a prescribed plate shape is possible for only one angle of attack of the plate. An advantage of this regime is that the drag force due to spray formation is equal to zero.

Wu & Whitney succeeded in obtaining an approximate analytical solution to the above problem for small values of the parameter $k = (L - l)/l$. We slightly modify their formulation, namely we assume that only the total arclength $2L$ is fixed and try to construct an exact analytical solution to this new problem. As we shall see later our solution to the modified problem turns out to be an exact solution to the initial one for a particular value of $k = \sinh(1) - 1 \approx 0.1752011$.

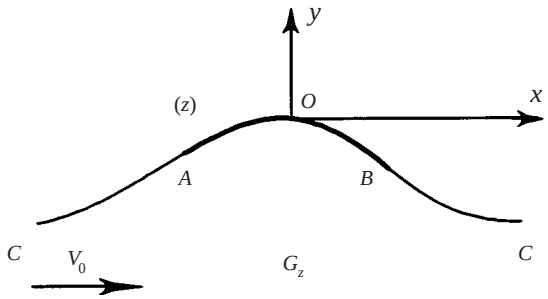

FIGURE 1. Flow region in the physical z-plane.

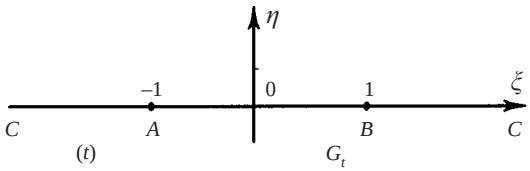

FIGURE 2. Parametric t-plane.

2. Mathematical formulations

As in Wu & Whitney (1972) we choose the lower half-plane G_t as a parametric t-plane (see figure 2). The conformal mapping of the domain G_t onto the region of the complex potential W is as follows:

$$W = aV_0 t, \tag{2.1}$$

where a is a positive constant, which has dimension of length.

We introduce the logarithmic hodograph variable

$$\omega(t) = \log \frac{V_0 \, \mathrm{d}z}{\mathrm{d}W} = \log \frac{V_0}{V} + \mathrm{i}\,\theta, \tag{2.2}$$

where V is the flow velocity, θ is the inclination of the velocity vector. Let us assume that the function

$$v(\xi) = \mathrm{Re}\,(\omega(t)) \quad \text{for} \quad t = \xi, \quad |\xi| \leqslant 1, \tag{2.3}$$

is known. On the free streamlines CA and BC we have

$$\mathrm{Re}\,(\omega(t)) = 0, \quad \text{for} \quad t = \xi, \quad |\xi| \geqslant 1. \tag{2.4}$$

With the Schwarz–Poisson formula we obtain from (2.3) and (2.4) that

$$\omega(t) = -\frac{1}{\pi\,\mathrm{i}} \int_{-1}^{1} \frac{v(\xi)\,\mathrm{d}\xi}{\xi - t}. \tag{2.5}$$

By means of formulae (2.1)–(2.5) all features of the flow can be completely determined in terms of $v(\xi)$ and a. In particular, for the total arclength $2L$ we have the representation

$$2L = a \int_{-1}^{1} \mathrm{e}^{v(\xi)}\,\mathrm{d}\xi. \tag{2.6}$$

For the total force $F = F_x + \mathrm{i}F_y$, consisting of the drag F_x and lift F_y, the following formulae hold (Wu & Whitney 1972):

$$F_y = \rho V_0^2 a \int_{-1}^{1} v(\xi)\,\mathrm{d}\xi, \qquad F_x = 0, \tag{2.7}$$

where ρ is the density of the fluid.

Up to this point we have reproduced the reasoning by Wu & Whitney (1972) to formulate the problem in terms of the function $v(\xi)$. Now we eliminate the parameter a from (2.6) and (2.7) to obtain

$$F_y = \rho V_0^2 L \mathscr{J}[v] \tag{2.8}$$

with

$$\mathscr{J}[v] = \frac{2\displaystyle\int_{-1}^{1} v(\xi)\,\mathrm{d}\xi}{\displaystyle\int_{-1}^{1} \mathrm{e}^{v(\xi)}\,\mathrm{d}\xi}. \tag{2.9}$$

Thus the hydrodynamic problem of maximizing the lift of the planing plate under the constraint of fixed arclength $2L$ is equivalent to finding the function $v(\xi)$ which maximizes the functional (2.9).

3. Finding the maximum lift force

Since for any $v(\xi) > 0$ the values of the functional $\mathscr{J}[v]$ are positive we shall seek its maximum under the assumption that the integral

$$T = \int_{-1}^{1} v(\xi)\,\mathrm{d}\xi$$

takes a positive value. We can estimate the positive denominator in (2.9) by a special case of Jensen's inequality (see e.g. Hardy, Littlewood & Polya 1934, p. 138):

$$\int_a^b f(\xi)\,\mathrm{e}^{v(\xi)}\,\mathrm{d}\xi \geqslant \exp\left[\int_a^b f(\xi)\,v(\xi)\,\mathrm{d}\xi\right], \tag{3.1}$$

where

$$\int_a^b f(\xi)\,\mathrm{d}\xi = 1, \quad f(\xi) \geqslant 0,$$

and the equal sign in (3.1) holds if and only if $v(\xi) \equiv \text{const}$. As $T > 0$ we apply (3.1) to the denominator in (2.9) to obtain

$$\mathscr{J}[v] \leqslant T\mathrm{e}^{-T/2}. \tag{3.2}$$

The right-hand side of the inequality (3.2) is a function of the T-argument. This function achieves its strongly positive maximum at $T = 2$. Therefore

$$\mathscr{J}[v] \leqslant 2\mathrm{e}^{-1}, \tag{3.3}$$

where the equal sign holds if and only if

$$v(\xi) \equiv 1. \tag{3.4}$$

Thus the function (3.4) is the solution to the problem posed. The values of the global

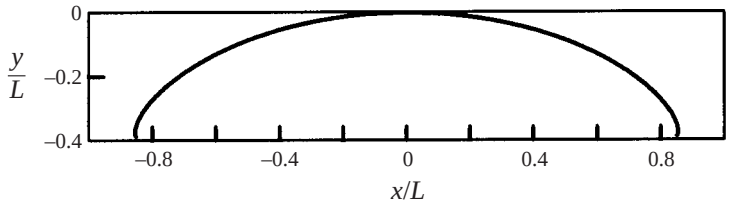

FIGURE 3. Shape of the maximum-lift plate.

maximum F_{ymax} and the function $\omega(t)$ can be written as

$$F_y \leqslant F_{ymax} = 2\rho V_0^2 L\,\mathrm{e}^{-1}, \tag{3.5}$$

$$\omega(t) = \frac{\mathrm{i}}{\pi}\log\frac{t-1}{t+1}. \tag{3.6}$$

The technique of applying Jensen's inequality to determining optimum profiles, which maximize hydrodynamic forces in free-surface flows, has been used earlier by Maklakov (1988), Maklakov & Uglov (1995). The technique allows one not only to find an exact analytical solution but also to prove that the solution gives the global extremum. By the simplicity of the problem considered in this work the technique takes here the simplest and clearest form.

From (3.4) and (3.6) we find that the inclination θ of the tangent to the optimum plate and the arclength s are connected by the formula

$$\theta = \frac{1}{\pi}\log\frac{1-s/L}{1+s/L}. \tag{3.7}$$

From (3.4) we deduce that the velocity along the optimum plate is constant: $V(s) = V_0\,\mathrm{e}^{-1}$. The domain corresponding to the flow region in the ω-plane is the vertical strip $0 \leqslant \mathrm{Re}\,(\omega) \leqslant 1$.

From (3.7) it follows that the optimum plate is symmetric with respect to the y-axes and in the vicinities of the end points A and B takes the form of spirals. By using (3.7), after a little algebra it is possible to show that the spirals are asymptotically logarithmic, and are described by the equation (for the right half of the optimum plate)

$$r/L = 2\,\exp(M + \pi\phi), \tag{3.8}$$

where $M = -\pi^2/2 - \pi\arctan\pi + \log[\pi/(\pi^2+1)^{1/2}]$, ϕ is a polar angle, r is the distance between a point on the optimum plate and the pole B of the spiral.

The shape of the optimum plate can be found from (3.7) and the formulae

$$x(s) = \int_0^s \cos\theta(s)\,\mathrm{d}s, \quad y(s) = \int_0^s \sin\theta(s)\,\mathrm{d}s. \tag{3.9}$$

This shape is shown in figure 3. Note that the spirals near the end points of the optimum plate are so tightly wound that they cannot be seen at any scales. Indeed, it follows from (3.8) that with every one-half revolution of the radius vector $\boldsymbol{r}$ its length decreases by the factor $\mathrm{e}^{-\pi^2} \approx 0.5 \times 10^{-4}$. Therefore, if we plot a part of the spiral corresponding to one-half revolution of the radius vector $\boldsymbol{r}$, the remaining part will look like a point at any scales.

4. Comparisons

Now we calculate the chord length $2l$ and the parameter $k = (L - l)/l$ for the optimum plate. From (3.7) and (3.9) we have

$$\frac{l}{L} = \frac{1}{2}\int_{-1}^{1} \cos\left(\frac{1}{\pi}\log\frac{1-\xi}{1+\xi}\right) \mathrm{d}\xi. \tag{4.1}$$

Making use of the transformation

$$u = \frac{1}{\pi}\log\frac{1-\xi}{1+\xi}$$

we obtain

$$\frac{l}{L} = \pi\int_{-\infty}^{\infty} \frac{\mathrm{e}^{\pi u}}{(1+\mathrm{e}^{\pi u})^2}\cos u\,\mathrm{d}u = \pi\,\mathrm{Re}\,(I),$$

where

$$I = \int_{-\infty}^{\infty} \frac{\mathrm{e}^{\pi u + \mathrm{i}u}}{(1+\mathrm{e}^{\pi u})^2}\,\mathrm{d}u.$$

The last integral can be calculated with the theory of residues by integrating the function $F(t) = \mathrm{e}^{\pi t+\mathrm{i}t}/(1+\mathrm{e}^{\pi t})^2$ along the boundaries of the strip $0 < \mathrm{Im}\,(t) < 2$ in the t-plane. The calculation gives

$$\frac{l}{L} = \frac{2\mathrm{e}}{\mathrm{e}^2-1}, \quad k = \sinh(1) - 1 \approx 0.1752011.$$

Dividing both sides of the inequality (3.5) by $\rho V_0^2 L$, we can see that the lift coefficient, based on the chord length, has the following estimate:

$$C_y = \frac{F_y}{\rho V_0^2 l} \leqslant 2\mathrm{e}^{-1}(1+k), \tag{4.2}$$

where the equal sign holds if and only if $k = \sinh(1) - 1$ and only for the plate whose shape is described by (3.7) and (3.9). So we have just obtained not only the exact analytical solution to the modified problem, but a full solution to the initial problem by Wu & Whitney (1972) for a particular value of the parameter $k = \sinh(1) - 1$.

For small values of k the work by Wu & Whitney (1972) presents the approximate analytical solution to the full problem given by the formulae

$$C_{ymax} = 4[2\mu\pi\cot(\mu\pi)]^{1/2}/l(\mu), \quad k = \cot^2(\mu\pi)\left(1 - \frac{\sin 2\mu\pi}{2\mu\pi}\right)/l(\mu) \tag{4.3}$$

with

$$l(\mu) = 4 - \frac{1}{\sin^2\mu\pi}\left(1 - \frac{\sin 2\mu\pi}{2\mu\pi}\right) + [8\mu\pi\cot(\mu\pi)]^{1/2}. \tag{4.4}$$

Line 1 in figure 4 demonstrates the function $C_{ymax}(k)$ given by (4.3) and (4.4). The straight line 2 in figure 4 is the estimating function (4.2). As one can see by comparing lines 1 and 2, the approximate analytical solution may be correct only for very small values of k and gives excessive values of the maximum lift for $k \geqslant 0.0200223$, the last value being the abscissa of the point where line 2 intersects line 1.

Besides the approximate analytical solution Wu & Whitney (1972) proposed a technique based on the Fourier-series expansion of the function to be found. In carrying out the calculation they kept only two terms in the series. Line 3 in figure 4 shows the function $C_{ymax}(k)$ obtained in Wu & Whitney (1972) by the two-term

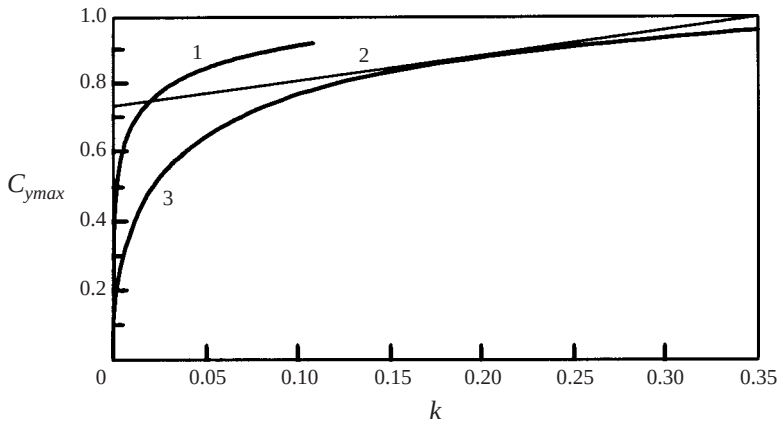

FIGURE 4. C_{ymax} versus k: curve 1, analytical method by Wu & Whitney (1972) for small values of k; 2, estimate (4.2); 3, approximate method by Wu & Whitney (1972) based on a two-term Fourier expansion.

expansion. By comparing lines 2 and 3 it is possible to deduce that the numerical result by Wu & Whitney is in excellent agreement with our exact result in the vicinity of point $k = 0.1752011$. The straight line 2 practically touches line 3. It is worth noting that the two-term expansion does not give any singularities for the end points A and B and as a consequence does not give any spirals. Therefore, based upon the agreement of the two results, the contribution of the spirals to the lift force seems to be small.

5. Realizable profile shapes

A disturbing feature of the solution (3.4), obtained in § 3, is the discontinuity of the velocity field at the end points of the optimum plate. Indeed, on the free streamlines CA and BC we have $V = V_0$, whereas at the end points A and B on the optimum plate $V = \mathrm{e}^{-1}V_0$. On the one hand the discontinuity leads to the technically unrealizable profile shape with spirals, on the other hand the discontinuity gives rise to an infinite pressure gradient at the leading edge and, as a consequence, to inevitable separation. But as follows from § 4 the contribution of the spirals to the lift force seems to be small, and the most natural way to remove the discontinuity seems to be to cut off small segments of the optimum plate near its ends. The lengths of the removed segments must be small enough not to lead to a considerable change in the lift force, and at the same time must be large enough not to lead to a very unfavourable pressure gradient near the leading edge or to a technically unrealizable shape near the trailing edge. To answer the question of whether such a compromise is possible the technique of solving the problem on planing plates with prescribed shapes needs to be developed.

Let the shape of a convex plate AB be given by the equation

$$M\,\mathrm{d}\theta/\mathrm{d}s = K(\theta), \quad T_{min} \leqslant \theta \leqslant T_{max}, \tag{5.1}$$

where $K(\theta)$ is a given non-vanishing function, T_{min} and T_{max} define the location of the ends of the plate. The stretch factor M defines the total arclength of the plate. In

our case the total arclength equals $2L$ and

$$M = 2L\left(\int_{T_{max}}^{T_{min}} \frac{\mathrm{d}\theta}{K(\theta)}\right)^{-1}. \tag{5.2}$$

Let us introduce the function

$$\lambda(\xi) = \mathrm{d}\theta/\mathrm{d}\xi, \quad |\xi| \leqslant 1,$$

and assume that $\lambda(\xi)$ is known. Then we can find

$$\mathrm{Im}\,(\omega(t)) = \theta(\xi) = T_{max} + \mathscr{U}[\lambda] \quad \text{for} \quad t = \xi, \quad |\xi| \leqslant 1, \tag{5.3}$$

where

$$\mathscr{U}[\lambda] = \int_{-1}^{\xi} \lambda(\sigma)\,\mathrm{d}\sigma. \tag{5.4}$$

The conditions (2.4) and (5.3) constitute a mixed boundary value problem for the analytic function $\omega(t)$, and $\omega(t)$ can be restored by the formula

$$\omega(t) = \frac{(t^2-1)^{1/2}}{\pi\,\mathrm{i}} \int_{-1}^{1} \frac{\theta(\sigma)\,\mathrm{d}\sigma}{(1-\sigma^2)^{1/2}(\sigma - t)}. \tag{5.5}$$

It follows from (5.5) that

$$v(\xi) = -\frac{(1-\xi^2)^{1/2}}{\pi} \int_{-1}^{1} \frac{\theta(\sigma)\,\mathrm{d}\sigma}{(1-\sigma^2)^{1/2}(\sigma - \xi)} = \mathscr{C}[\theta], \quad |\xi| \leqslant 1, \tag{5.6}$$

where $\mathscr{C}[\theta]$ is a singular linear operator.

Now by making use of (5.1), (5.3), (5.6) and standard approaches (see Birkhoff & Zarantonello 1957) we can deduce a nonlinear equation to find the function $\lambda(\xi)$:

$$\lambda(\xi) = \alpha K(T_{max} + \mathscr{U}[\lambda]) \exp(\mathscr{C}\mathscr{U}[\lambda]) \tag{5.7}$$

with $\alpha = a/M$. To find the parameter α we should add to (5.7) the relationship

$$\int_{-1}^{1} \lambda(\sigma)\,\mathrm{d}\sigma = T_{min} - T_{max}. \tag{5.8}$$

Equations (5.7) and (5.8) represent the system of coupled equations to determine $\lambda(\xi)$ and α. We solve the system (5.7) and (5.8) numerically by means of discretization and Newton's iterative procedure. The details of the numerical technique can be found in the Appendix.

In the case of the plate given by (3.7) and (3.9) the function $K(\theta)$ takes the form

$$K(\theta) = -\frac{2}{\pi}\cosh\frac{\pi\theta}{2}.$$

If $T_{min} = -\infty, T_{max} = +\infty$, then according to (5.2) the factor $M = L$ and we deal with the plate shown in figure 3. If T_{min} and T_{max} take finite values, then we deal only with a part of the plate shown. First we consider symmetric parts choosing $T_{max} = -T_{min}$. The velocity distributions along these parts are shown in figure 5. These velocity distributions demonstrate very explicit non-uniform convergence to the function $V/V_0 = \mathrm{e}^{-1} \approx 0.3679$.

In table 1 we show the lift coefficients C_L, based on the total arclength $2L$, for the optimum plate with symmetrically removed segments. It follows from (3.5) that $C_L = F_y/(\rho V_0^2 L) \leqslant C_{Lmax} = 2\mathrm{e}^{-1}$. As one can see from column 3 of table 1 the lift

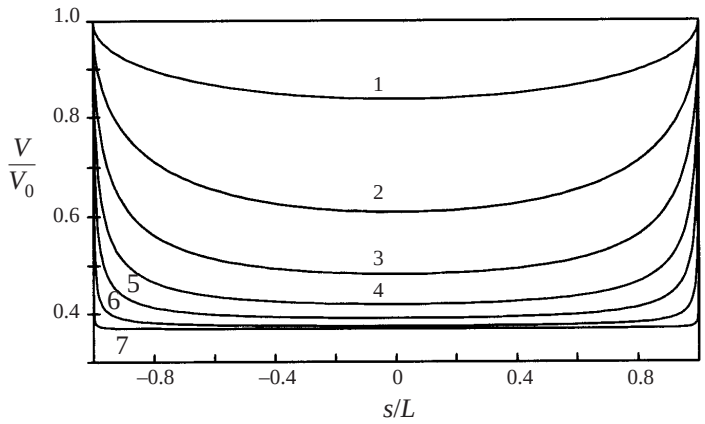

FIGURE 5. Symmetric case. Velocity distributions along the parts of the optimum plate: curve 1, $T_{max} = 10°$; 2, $T_{max} = 30°$; 3, $T_{max} = 50°$; 4, $T_{max} = 70°$; 5, $T_{max} = 90°$; 6, $T_{max} = 120°$; 7, $T_{max} = 180°$.

No.	T_{max} (deg.)	$C_L e/2$	C_D	S_{tran}/L	S_{sep}/L	C_L/C_D
1	10	0.3260	0.0028	−0.8787	1.000	85.47
2	30	0.7277	0.0028	−0.9416	1.000	189.1
3	50	0.9020	0.0027	−0.9801	1.000	241.7
4	70	0.9670	0.0027	−0.9944	1.000	264.4
5	90	0.9892	0.0027	−0.9982	1.000	270.4
6	120	0.9980	0.0027	−0.9997	1.000	269.5
7	180	0.9999	—	−1.000	−1.000	—

TABLE 1. Symmetric case. Integral characteristics of the parts of optimum plate.

coefficients converge to the limiting value $2e^{-1}$. For $T_{max} = 90°$ the lift coefficient is only about 1% less than the maximum; for $T_{max} = 120°$ the difference between the maximum value and the obtained one is only 0.2%. Columns 5 and 6 of table 1 demonstrate the behaviour of boundary layer for the velocity distributions shown in figure 5. We calculate the boundary layer by means of Eppler's integral method (see Eppler 1990) assuming that it starts at the leading edge. The last assumption looks natural because the skin friction between water and air is much less than between water and a solid wall. The Reynolds number, defined by $Re = V_0 L/v$ (here v is the kinematic viscous coefficient), is taken to be equal to 10^7. In spite of the fact that velocity distributions shown in figure 5 have very unfavourable pressure gradients starting at the leading edge, the boundary layer does not separate even for curve 6 of figure 5, when $T_{max} = -T_{min} = 120°$. This is because the boundary layer starts at the leading edge without any history. But the unfavourable pressure gradient leads to the boundary layer quickly becoming turbulent and very close positions of the transition point s_{tran} to the leading edge. In column 4 of table 1 the drag coefficients $C_D = F_x/(\rho V_0^2 L)$ due to the skin friction are shown.

Since the pressure gradients for the velocity distributions shown in figure 5 are favourable near the trailing edge, there is no need to cut off small segments symmetrically. But for a non-symmetrical plate it needs to be taken into account that the

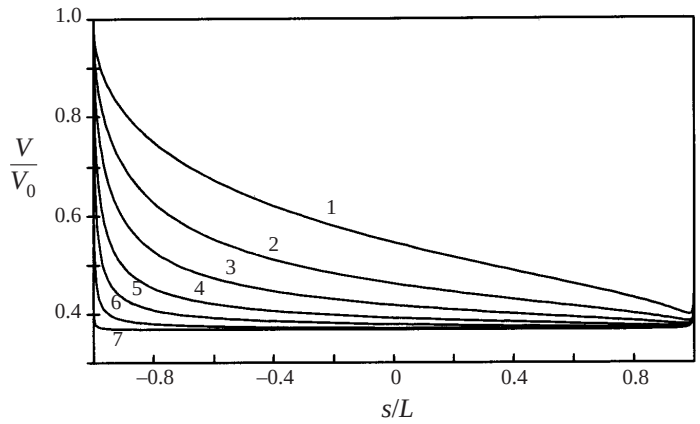

FIGURE 6. Non-symmetrical case. Velocity distributions along the parts of the optimum plate ($T_{min} = -180°$): curve 1, $T_{max} = 0°$; 2, $T_{max} = 30°$; 3, $T_{max} = 50°$; 4, $T_{max} = 70°$; 5, $T_{max} = 90°$; 6, $T_{max} = 120°$; 7, $T_{max} = 180°$.

No.	T_{max} (deg.)	$C_L e/2$	C_D	S_{tran}/L	S_{sep}/L	C_L/C_D	α_a (deg.)
1	0	0.8364	0.0021	−0.9322	1.000	299.0	−28.33
2	30	0.9243	0.0022	−0.9561	1.000	314.7	−11.71
3	50	0.9656	0.0023	−0.9843	1.000	309.5	−5.71
4	70	0.9865	0.0025	−0.9948	1.000	295.9	−2.57
5	90	0.9951	0.0026	−0.9983	1.000	283.6	−1.08
6	120	0.9990	0.0027	−0.9997	1.000	272.5	−0.27
7	180	0.9999	—	−1.000	−1.000	—	0

TABLE 2. Non-symmetrical case. Integral characteristics of the parts of the optimum plate ($T_{min} = -180°$).

function $\omega(t)$ is not necessary zero at infinity, namely

$$\omega(\infty) = \mathrm{i}\,\alpha_a = \frac{\mathrm{i}}{\pi}\int_1^1 \frac{\theta(\sigma)\,\mathrm{d}\sigma}{(1-\sigma^2)^{1/2}},$$

where α_a is the angle by which we need to rotate the plate, defined by (5.1), in the clockwise direction to satisfy the smooth entry condition. Now we choose $T_{min} = -180° = \text{const}$, and change T_{max}. The velocity distributions along the plates obtained are shown in figure 6. In figure 6 one can also see non-uniform convergence of the function $V(s)/V_0$ to $V(s)/V_0 = \mathrm{e}^{-1}$.

In table 2 integral characteristics of the calculated plates are demonstrated. The last column shows the angles of rotation α_a. As one can see from table 2 for $T_{max} = 90°$ we have a lift coefficient which is only 0.5% less than the maximum; for $T_{max} = 120°$ the difference is 0.1%. As in the previous symmetric case we have no separation of the boundary layer for $Re = 10^7$ and $T_{max} \leqslant 120°$. For $T_{max} = 120°$ the lift-to-drag ratio in the non-symmetrical case is about 270 as in the symmetric one, but for $T_{max} = 30°$ the ratio is greater and achieves a value of 315. This means that a non-symmetrical part of the optimum plate can give a greater lift-to-drag ratio than almost the entire optimum plate with $T_{max} = 120°$. It seems to be possible to formulate and solve the problem of finding the planing plate that maximizes the lift-to-drag ratio.

6. Conclusions

The optimum shape of a planing surface found analytically in an ideal fluid and defined by (3.7) and (3.9), turns out to be technically unrealizable because of small, tightly wound spirals near the end points. Comparison with the numerical results by Wu & Whitney (1972) suggests that there exist realizable shapes without spirals which have the lift coefficients almost as high as the maximum. In § 5 it is shown numerically that if small segments are cut off near the ends of the 'ideal' optimum plate, the remaining part, which satisfies the condition of continuity of the velocity field, can give a lift which is only 0.1% less than the maximum and at the same time the boundary layer along the part does not separate. This means that the problem solved can be reformulated as follows: find the planing plate of fixed arclength $2L$ that maximizes the lift force under the restriction that for a fixed Reynolds number $Re = V_0 L/\nu$ the boundary layer along the plate will be non-separating.

We would like to acknowledge the useful comments of referees that stimulated writing § 5. This work was supported by the Russian Foundation of Basic Research under Grants 96-01-00111, 96-01-00123.

Appendix. Numerical method

To obtain a nonlinear solution to (5.7) and (5.8) it is necessary to resort to a numerical method. The mesh of discrete ξ-points on the segment $[-1, 1]$ is defined by

$$\xi_i = -1 + 2P(u_i), \quad P(u) = u^4(35 - 84u + 70u^2 - 20u^3),$$
$$u_i = \frac{(i-1)}{(N-1)}, \quad i = \overline{1, N}, \tag{A 1}$$

where N is the number of collocation points, and the polynomial $P(u)$ is chosen so that

$$P(1) = 1, \quad P(0) = P'(0) = P''(0) = P'''(0) = P'(1) = P''(1) = P'''(1) = 0.$$

The objective of the numerical method is to find the $\lambda(\xi_i)$. The nodes ξ_i of the mesh (A 1) are strongly concentrated near the end points of the segment $[-1, 1]$, and this concentration is necessary to catch large derivatives of the function $\lambda(\xi)$ near these points.

To discretize (5.7) and (5.8) we need to construct discrete analogues of the linear operators $\mathscr{U}[\lambda]$ and $\mathscr{C}\mathscr{U}[\lambda]$. We will seek the values of these operators on the mesh ξ_i in the form

$$\mathscr{U}[\lambda](\xi_i) = \sum_{j=1}^{N} U_{ij}\lambda_j, \quad \mathscr{C}\mathscr{U}[\lambda](\xi_i) = \sum_{j=1}^{N} D_{ij}\lambda_j, \quad i = \overline{1, N},$$

where the coefficients U_{ij}, D_{ij} depend only on the location of the nodes ξ_i and the technique that we choose for approximate integration on a fixed mesh. In developing this technique we always obey the following rule: if an integrand has no singularity, approximate it by the natural cubic spline (the second derivative at the end points equals zero) and after that integrate the cubic spline analytically.

On doing so the columns of the square matrix (U_{ij}) can be found in the following manner. Specify the index j of a column and calculate a so-called fundamental spline (see Ahlberg, Nilson & Walsh 1967). At the points ξ_i the values of this spline equal

zero, except the value at the point ξ_j, which equals unity. By integrating in sequence the fundamental spline from -1 to ξ_i find the column $U_{ij}, i = \overline{1, N}$.

To calculate $\int_{-1}^{1} f(\xi)/(\xi^2 - 1)^{1/2}\,\mathrm{d}\xi$, where $f(\xi)$ is a smooth function, we will seek the integral in the form

$$\int_{-1}^{1} \frac{f(\xi)\,\mathrm{d}\xi}{(\xi^2 - 1)^{1/2}} = \sum_{j=1}^{N} \alpha_j f_j, \tag{A 2}$$

where α_j are coefficients that we need to find, and $f_j = f(\xi_j)$. To remove the singularities in the integrand we make the transformation $u = -\arccos\xi$. This leads to a new mesh

$$u_i = -\arccos\xi_i, \quad i = \overline{1, N}, \quad -\pi \leqslant u_i \leqslant 0.$$

Integrating the fundamental splines, constructed on the mesh u_i, from $-\pi$ to zero, we find sequentially the coefficients α_j.

Taking into account that

$$\int_{-1}^{1} \frac{\mathrm{d}\sigma}{(1 - \sigma^2)^{1/2}(\sigma - \xi)} = 0, \tag{A 3}$$

we can represent the operator $\mathscr{C}[\theta]$ in the form

$$\mathscr{C}[\theta] = -\frac{(1 - \xi^2)^{1/2}}{\pi} \int_{-1}^{1} \frac{[\theta(\sigma) - \theta(\xi)]\,\mathrm{d}\sigma}{(1 - \sigma^2)^{1/2}(\sigma - \xi)}. \tag{A 4}$$

By means of (A 2), (A 4) after a little algebra we deduce the following representation for the coefficients D_{ij}:

$$D_{ij} = -\frac{(1 - \xi_i^2)^{1/2}}{\pi} \begin{cases} \displaystyle\sum_{k=1}^{N} E_{ik} U_{kj}, & i \neq j, \\ \displaystyle\sum_{k=1}^{N} E_{ik} U_{kj} + \alpha_i, & i = j, \end{cases}$$

$$E_{ij} = \begin{cases} \alpha_j/(\xi_j - \xi_i), & i \neq j, \\ \displaystyle -\sum_{\substack{k=1 \\ k \neq i}}^{N} \alpha_k/(\xi_k - \xi_i), & i = j, \end{cases}$$

where $i = \overline{1, N}, j = \overline{1, N}$, and (E_{ij}) is an auxiliary square matrix.

As the coefficients U_{ij}, D_{ij} are found, the discrete analogue of the system (5.7) and (5.8) appears as follows:

$$\lambda_i = \alpha K \left(T_{max} + \sum_{j=1}^{N} U_{ij}\lambda_j \right) \exp\left(\sum_{i=1}^{N} D_{ij}\lambda_j \right), \quad i = \overline{1, N}, \tag{A 5}$$

$$\sum_{j=1}^{N} U_{Nj}\lambda_j = T_{min} - T_{max}. \tag{A 6}$$

This is the system of $N + 1$ equations with $N + 1$ unknowns that we solve by Newton's iterative procedure. The square matrices (U_{ij}) and (D_{ij}) depend only on N and can therefore be tabulated before the beginning of the iterations. The form of

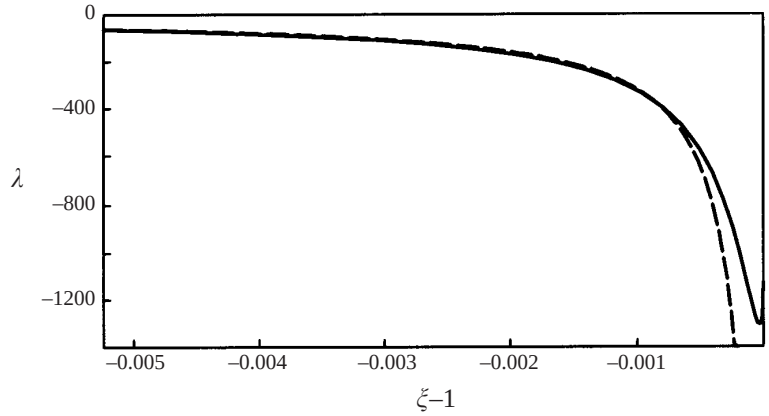

FIGURE 7. The functions $\lambda(\xi)$ for $T_{max} = -T_{min} = 180^\circ$ (solid line) and (A 7) (dashed line) near the point $\xi = 1$.

the equations (A 5) and (A 6) allows us to calculate the Jacobian 'derivative matrix' analytically, which makes the iterative cycle both quicker and more precise.

The above technique can be applied to many free-surface problems with prescribed curvilinear boundaries. Its main advantage in comparison with the technique of the truncated Fourier series (see e.g. Birkhoff & Zarantonello 1957) is the possibility of using non-uniform meshes. Indeed, let us consider the function $\lambda(\xi)$ for $T_{min} = T_{max} = 180^\circ$, shown in figure 7 near the point $\xi = 1$ by a solid line. For these T_{min} and T_{max} the function $\lambda(\xi)$ must be close to

$$\lambda_{opt}(\xi) = \frac{\mathrm{d}}{\mathrm{d}\xi}\left[\frac{1}{\pi}\log\frac{\xi-1}{\xi+1}\right] = \frac{2}{\pi}\frac{1}{\xi^2-1} \tag{A 7}$$

everywhere except small segments near the end points $\xi = -1$ and $\xi = 1$, where $\lambda(\xi)$ and $\lambda_{opt}(\xi)$ take very significant negative values. The function (A 7) is shown in figure 7 by a dashed line. As one can see from figure 7 the non-uniform mesh, defined by (A 1), allows us to capture the behaviour of $\lambda(\xi)$ near the end points, including the local minimum located approximately at $\xi = 0.999974$. It is evident that to capture this minimum by a uniform mesh we need to take

$$N > 2/(1 - 0.999974) \approx 76923.$$

In our calculations we took $N = 301$.

REFERENCES

AHLBERG, J. H., NILSON, E. N. & WALSH, J. L. 1967 *The Theory of Splines and their Applications.* Academic.

BIRKHOFF, G. & ZARANTONELLO, E. 1957 *Jets, Wakes and Cavities.* Academic.

CUMBERBATCH, E. 1958 Two-dimensional planing at high Froude number. *J. Fluid Mech.* **4**, 486.

EPPLER, R. 1990 *Airfoil Design and Data.* Springer.

HARDY, G., LITTLEWOOD, J. & POLYA, G. 1934 *Inequalities.* Cambridge University Press.

MAKLAKOV, D. V. 1988 On the maximum drag of a curved obstacle in a flow with detachment of jets. *Dokl. Akad. Nauk SSSR* **298**, N3, 574–577 (in Russian).

MAKLAKOV, D. V. & UGLOV, A. N. 1995 On the maximum drag of a curved plate in flow with a wake. *Eur. J. Appl. Math.* **6**(5), 517–527.

WU, T. Y. & WHITNEY, A. K. 1972 Theory of optimum shapes in free-surface flows. Part 1. Optimum profile on sprayless planing surface. *J. Fluid Mech.* **55**, 439–455.